Interfacial Fabrication of Supramolecular Polymer Networks Using Mussel-Inspired Catechol-Iron Complexes

Kaijuan Li[1], Yunhui Wen[1], Zhiqin Xia[1], Zhao Zhang[1], Jiang Liu[1], Thomas P. Russell[3,4] and Shaowei Shi[1,2]*

[1]Beijing Advanced Innovation Center for Soft Matter Science and Engineering & College of Materials Science and Engineering, Beijing University of Chemical Technology, Beijing 100029, China

[2]Beijing Engineering Research Center for the Synthesis and Applications of Waterborne Polymers, Beijing University of Chemical Technology, Beijing 100029, China

[3]Department of Polymer Science and Engineering, University of Massachusetts, Amherst, Massachusetts 01003, USA

[4]Materials Sciences Division, Lawrence Berkeley National Laboratory, 1 Cyclotron Road, Berkeley, California 94720, USA

KEYWORDS: Supramolecular polymers, interfacial polymerization, dynamic chemistry, responsiveness, composite membranes

ABSTRACT: The liquid-liquid interface provides a promising platform to construct supramolecular polymers and materials with advanced functions. However, supramolecular polymerization at the interface usually requires monomers with different or even orthogonal solubilities, which significantly limits the number of usable monomers. Here, we report a new strategy to construct supramolecular polymer networks at the oil-water interface using a water-soluble catechol-iron complex and an oil-soluble di-end-functionalized polymer. Owing to the dynamic catechol-iron coordination bond and imine bond, the resulting supramolecular polymer networks demonstrate excellent dynamic features and responsiveness to different stimuli including pH, redox, competing ligands and temperature. With asupramolecular polymer network serving as a building block, emulsions and 2D films can be generated that have potential applications in encapsulation, release and molecular separation.

Introduction

Supramolecular polymer systems constructed by directional and reversible noncovalent bonds have attracted much attention in the past few decades.[1-7] In view of the dynamic nature of noncovalent interactions, such as hydrogen bonding, host-guest interactions, π-π interactions and metal coordination, supramolecular polymers show many intriguing features including stimuli-responsiveness, degradability and self-healing, making them exceptional candidates for adaptive or smart materials.[8-14] In comparison to supramolecular polymers prepared in a homogeneous medium, supramolecular polymers prepared at the interface between two immiscible liquids, e.g., oil-water interface, are expected to have higher molecular weights and promising potential

for the generation of supramolecular polymeric films and microcapsules.[15-17] For the interfacial fabrication of supramolecular polymers, two strategies: supramolecular polymerization of covalent monomers at the liquid-liquid interface and covalent polymerization of supramonomers at the liquid-liquid interface, have been developed.[18] To the best of our knowledge, the noncovalent interactions used in the supramolecular interfacial polymerization are limited to cucurbit[8]uril (CB[8])-mediated host–guest interactions and hydrogen bonding. Extending the fabrication of supramolecular polymers with tunable structures, multiple stimuli-responsiveness and advanced functions at the liquid-liquid interface is needed.

Dynamic catechol-iron chemistry is correlated to the hardness and high extensibility of the cuticle of mussel byssal threads and suggested to impart self-healing properties.[19-22] The stability constants of tris- and bis-catechol-Fe^{3+} complexes are among the highest values of metal-ligand chelates, and the catechol-Fe^{3+} coordination can respond to different stimuli.[23-25] Using catechol-Fe^{3+} complexes as cross-linkers, dynamic cross-linked polymer networks, including hydrogels and bulk systems, have been developed that exhibit excellent mechanical, self-healing and responsive properties.[26-29] Inspired by the remarkable features of catechol-Fe^{3+} complexes, it is highly desirable to design and construct catechol-Fe^{3+} complex-based supramolecular polymers at the liquid-liquid interface, where the multiple stimuli-responsiveness and excellent mechanical properties are expected to be integrated.

In this work, by using an aqueous solution of tris-catechol-Fe^{3+} complex, PA_3/Fe(III), as a supramolecular cross-linker (prepared through the coordinative interactions between protocatechualdehyde (PA) and Fe^{3+}), and a toluene solution of difunctional polydimethylsiloxane end-capped with primary amines (NH_2-PDMS-NH_2), we generated

supramolecular polymer networks at the oil-water interface, where both Schiff-base bonds and metal-coordination bonds are introduced (Figure 1). The kinetics of the supramolecular polymerization at the interface is investigated by pendant drop tensiometry. Due to the dynamic nature of the catechol-Fe^{3+} complexes, the interfacial polymers are responsive to multiple stimuli, including pH, redox, competing ligands, and temperature, leading to a controllable assembly/jamming-to-disassembly/unjamming transition of the interfacial networks. Moreover, using an emulsion interface or a flat oil-water interface as a template, stable emulsion droplets and large area, defect-free supramolecular films can be successfully produced.

Results and Discussion

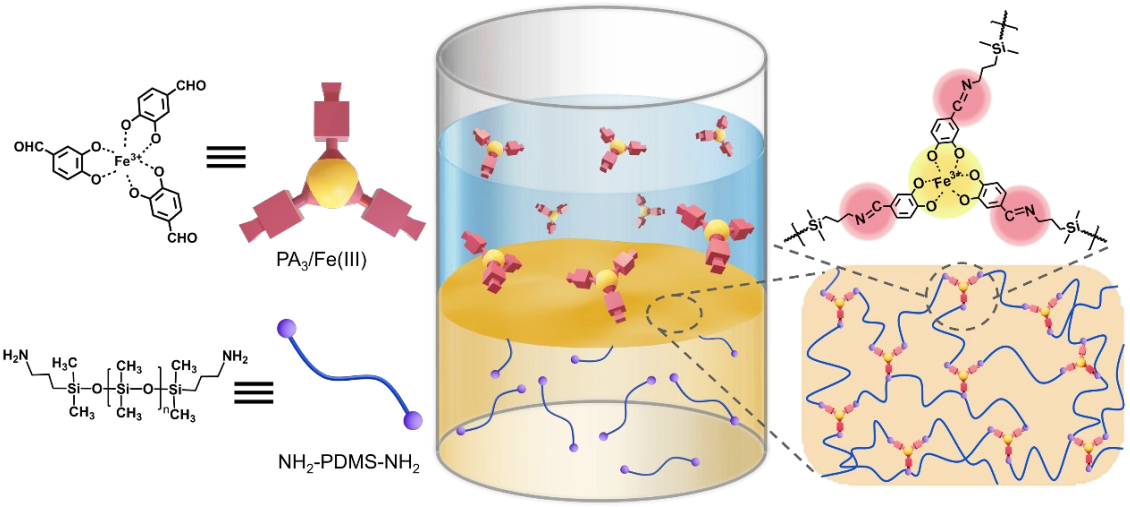

Figure 1. Schematics showing the interfacial fabrication of supramolecular polymer networks using PA_3/Fe(III) and NH_2-PDMS-NH_2.

Catechol-Fe^{3+} complexes were synthesized as described in the literature (Figure S1).[25] Dissolving catechol-Fe^{3+} complexes in water and NH_2-PDMS-NH_2 (M_n = 3000 g mol^{-1}) in toluene generates supramolecular polymers *in situ* at the interface. Since the stoichiometry of

catechol-Fe^{3+} complexes (mono-, bis-, or tris-) is controlled by pH by the deprotonation of the catechol hydroxyls, the architecture of the supramolecular polymer at the interface can be manipulated from from being linear to a network. As shown in Figure 2a-b, with decreasing pH, a chemical structureal evolution of the catechol-Fe^{3+} complexes from PA_3/Fe(III) (pH > 8.0) to bis-catechol-Fe^{3+} complex (PA_2/Fe(III), pH ~ 5.0-8.0), then to mono-catechol-Fe^{3+} complex (PA_1/Fe(III), pH < 5.0) is achieved,[30] as evidenced by the color change of catechol-Fe^{3+} complex-containing aqueous solutions and related UV−Vis absorption spectra (Figure S2). The kinetics of the supramolecular polymerization at the interface was investigated by tracking the dynamic interfacial tension (γ) using pendant drop tensiometry. The interfacial tensions of PA_3/Fe(III), PA_2/Fe(III), PA_1/Fe(III) and NH_2-PDMS-NH_2 at the toluene-water interface were investigated iniitally. As shown in Figure 2c and Figure S3, with PA_3/Fe(III), PA_2/Fe(III), or PA_1/Fe(III) dissolved in water against pure tolueue, the equilibrium interfacial tension range from 30.9 - 33.7 mN m^{-1}, close to that of the pure toluene-water system (35.8 mN m^{-1}, Figure S4), indicating the catechol-Fe^{3+} complexes are not interfacially active. NH_2-PDMS-NH_2, on the other hand, behaves as a surfactant and shows pH-dependent interfacial activity (Figure 2d and Figure S5). Since the pK_a of amine group is ~ 9.0, as the pH decreases, more amine groups can be protonated, increasing the surfactancy of NH_2-PDMS-NH_2 and further reducing the interfacial tension. We note that, at pH < 4.0, the interfacial tension is so low that the droplet falls from the needle, since the energy cost of distending the droplet is lower than the gravitational force pulling the droplet down.

Since the imine bonds formed by amine and aldehyde groups are unstable at acid conditions,[31] the interfacial polymerization is triggered at two pH conditions (8.6 or 6.2), where PA_3/Fe(III) or

PA_2/Fe(III) act as a cross-linker or linker, respectively. As shown in Figure 2e-f, with PA_3/Fe(III) or PA_2/Fe(III) dissolved in water and NH_2-PDMS-NH_2 dissolved in toluene, a low interfacial tension of ~ 12 mN m^{-1} was obtained after 1200 s, indicating the formation of supramolecular polymer networks or linear polymers at the interface. However, when reducing the volume of the droplet to compress the interfacial assemblies, different behaviors are observed. In the case of PA_3/Fe(III), wrinkles develop immediately on the droplet surface upon very small compression and cannot fully relax after 10 min, while the droplet retains its highly nonequilibrium shape (Figure S6 and Video S1), indicating the surface coverage (as estimated from the volume at which wrinkles appear relative to the initial volume)[32] of supramolecular polymer networks is very high and, when they are jammed at the interface, the degree of reorganization of polymer chains is low. On the other hand, when using PA_2/Fe(III) to form supramolecular linear polymers at the interface, wrinkles appear after a certain degree of compression and can fully relaxed in 3.0 min (Figure S7 and Video S2). This compression-relaxation can be repeated until the areal density of supramolecular linear polymers is too high (Figure S8). These results demonstrate that, with PA_3/Fe(III) as the cross-linker, the chain mobility at the interface can be significantly decreased, leading to a more "solid-like" interfacial film. It should be noted that, since all the pendant droplet experiments are performed at the room temperature, the effects of bond exchange of catechol-Fe^{3+} coordination and imine on relaxing the interfacial stress are ignored.[23, 33] We also performed control experiments where the PA monomer was dissolved in water (pH = 8.6 or 6.2) and NH_2-PDMS-NH_2 was dissolved in toluene (Figure S9). No wrinkles are observed when compressing the interfacial assemblies, indicating the binding energy of the PA-PDMS-PA or PA-PDMS-NH_2 at the interface is not sufficient to hold them at the interface under

compression, absent supramolecular polymer networks or linear polymers are formed at the interface.

The logarithmic representation of the interfacial tension in Figure 2g points to three different stages of the supramolecular interfacial polymerization. Iitially, a rapid reduction in the interfacial tension is seen, due to the diffusion of NH_2-PDMS-NH_2 to the interface and the subsequent interfacial polymerization. For the PA_2/Fe(III)-based system (pH = 6.2), the initial reduction in the interfacial tension is greater than that of PA_3/Fe(III)-based system (pH = 8.6) corresponding to the greater interfacial activity of NH_2-PDMS-NH_2 at lower pH. With time, a second slower process is observed, giving rise to a continued decrease in the interfacial tension, which can be attributed to the polymer growth at the interface. In comparison to PA_2/Fe(III)-based system, the reduction in the interfacial tension in PA_3/Fe(III)-based system is greater, as a result of the increased functional groups in PA_3/Fe(III). In the last stage, where the interfacial tension remains almost unchanged, polymerization may continue but mainly occurs at defects or thinner parts of the interfacial assemblies, similar to the conventional interfacial polymerization process.[34, 35]

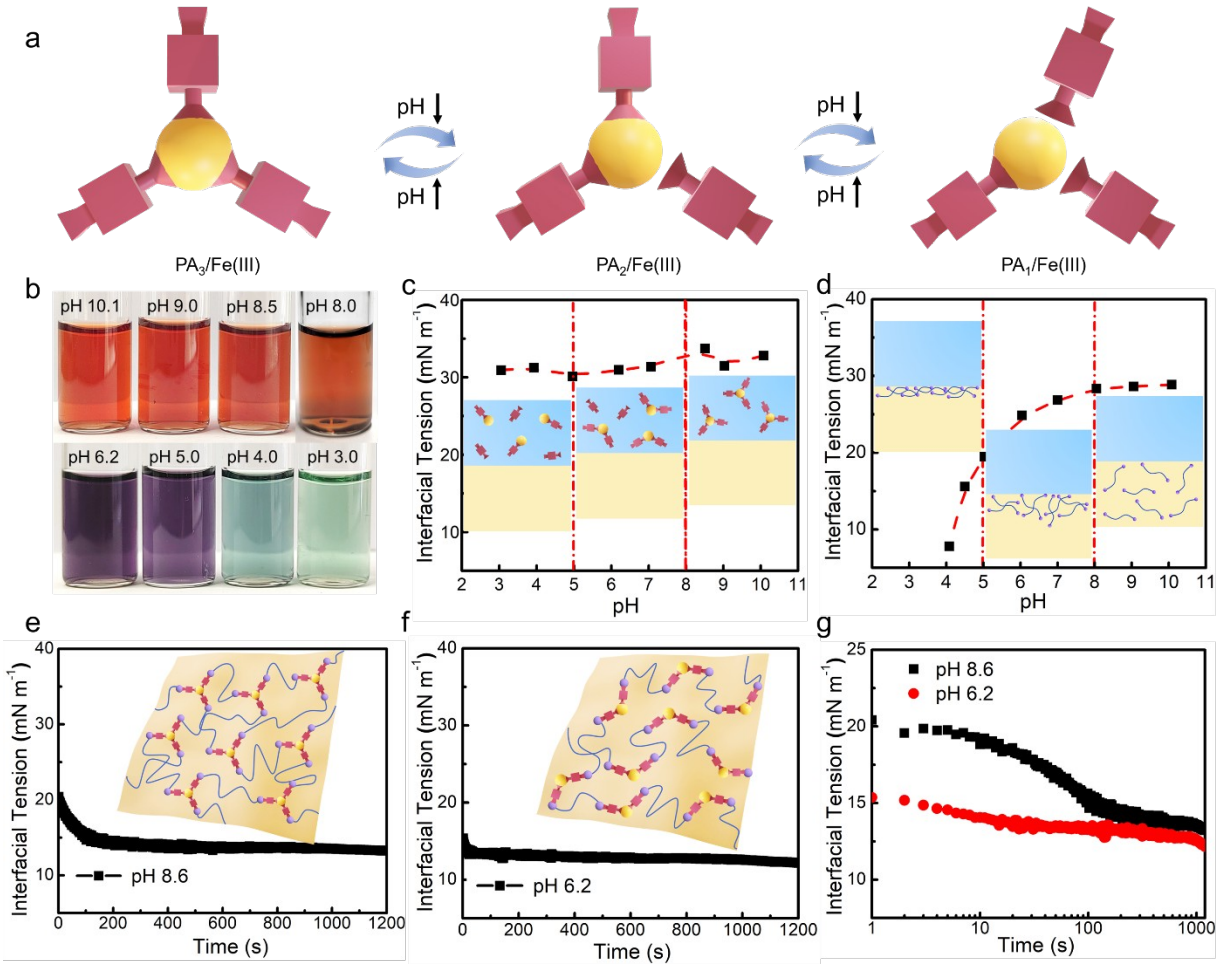

Figure 2. (a) Schematics showing the state of catechol-Fe^{3+} complex at different pH. (b) Color change of catechol-Fe^{3+} complex-containing aqueous solution at different pH; [catechol-Fe^{3+}] = 0.10 mg mL^{-1}. (c) Equilibrium interfacial tension of water-toluene systems with only catechol-Fe^{3+} complex dissolved in water at different pH; [catechol-Fe^{3+}] = 0.10 mg mL^{-1}. (d) Equilibrium interfacial tension of water-toluene systems with only NH_2-PDMS-NH_2 dissolved in toluene at different pH; [NH_2-PDMS-NH_2] = 1.0 mg mL^{-1}. (e) Time evolution of interfacial tensions of water-toluene system with PA_3/Fe(III) dissolved in water and NH_2-PDMS-NH_2 dissolved in toluene; [PA_3/Fe(III)] = 0.10 mg mL^{-1}, [NH_2-PDMS-NH_2] = 1.0 mg mL^{-1}, pH = 8.6. (f) Time evolution of interfacial tensions of water-toluene system with [PA_2/Fe(III)] dissolved in water

and NH_2-PDMS-NH_2 dissolved in toluene; [PA_2/Fe(III)] = 0.10 mg mL^{-1}, [NH_2-PDMS-NH_2] = 1.0 mg mL^{-1}, pH = 6.2. (g) Logarithmic representation of the data in (e) and (f).

The mechanical strength of interfacial films can be demonstrated by brining two droplets encapsulated with catechol-Fe^{3+} complex-based supramolecular polymers into contact. As shown in Figure 3a, with PA_3/Fe(III)-based supramolecular polymer networks at the interface (pH = 8.6), in a repeated contacting experiment (> 10 times), no coalescence is observed and droplets can be fully separated after the forced physical contact (Video S3). However,], with PA_2/Fe(III)-based supramolecular linear polymers at the interface (pH = 6.2), the two droplets do not coalesce after the first several contact experiments but, after repeated contacts, coalescences occurs indicating a decrease in the mechanical strength of the interfacial films (Figure 3b and Video S4). To quantify the mechanical properties of the supramolecular polymers, the interfacial rheological properties were investigated at low concentrations of catechol-Fe^{3+} complex and NH_2-PDMS-NH_2, by using an oscillating pendant drop and measuring the in-phase and out-of-phase components of the interfacial tension. As shown in Figure 3c-d, in the frequency range of 0.01 to 1.0 Hz, with either supramolecular polymer networks (pH = 8.6) or linear polymers (pH = 6.2) formed at the interface, both viscous (E''(ω)) and elastic (E'(ω)) components are obtained, with the elastic part being the dominant component, demonstrating the elastic nature of the interfacial assemblies. In comparison to PA_2/Fe(III)-based supramolecular linear polymers, a significantly increased E'(ω) over the whole frequency range is obtained for PA_3/Fe(III)-based supramolecular polymer networks, further demonstrating that the mechanical strength of the interfacial assemblies can be enhanced by the crosslinking strategy. Moreover, in the case of PA_3/Fe(III)-based supramolecular polymer networks, when a water droplet encapsulated with

PA_3/Fe(III)-based supramolecular polymer networks is fully extracted into the needle and then re-injected to the initial volume, a highly deformed droplet far from the equilibrium state is achieved, demonstrating the potential to construct structured liquids that can be used in biphasic reactors and microfluidic devices (Figure 3e).[36, 37] In the following studies, to ensure the robustness of the interfacial assemblies, the pH of the aqueous phase is fixed at 8.6 unless specifically noted, in which the PA_3/Fe(III)-based supramolecular polymer networks are formed at the interface.

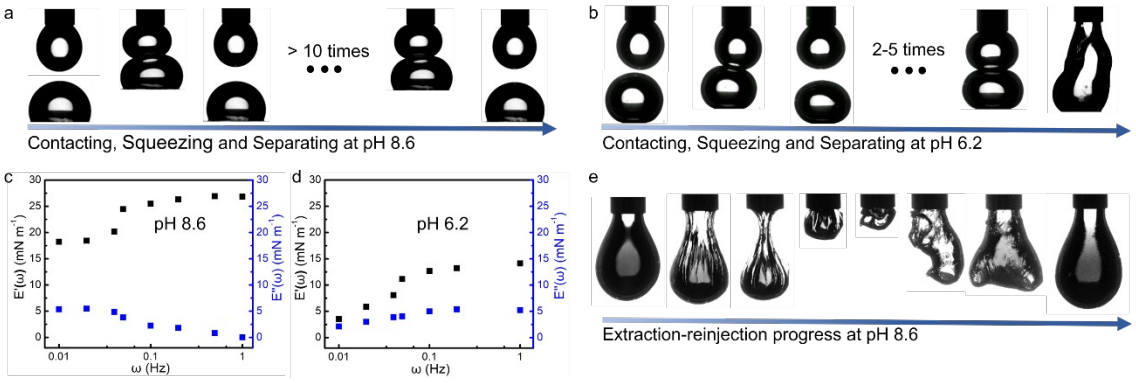

Figure 3. (a-b) Sequence of snapshots showing the process of contact, compression, and separation of two droplets of supramolecular polymer networks (left) and supramolecular linear polymers (right); [PA_3/Fe(III)] = 0.10 mg mL^{-1}, [PA_2/Fe(III)] = 0.10 mg mL^{-1}, [NH_2-PDMS-NH_2] = 1.0 mg mL^{-1}. (c-d) Storage and loss dilatational moduli, E′(ω) and E″(ω), of elastic films of supramolecular polymer networks (left) and supramolecular linear polymers (right); [PA_3/Fe(III)] = 0.02 mg mL^{-1}; [PA_2/Fe(III)] = 0.02 mg mL^{-1}; [NH_2-PDMS-NH_2] = 0.10 mg mL^{-1}; ω = 0.01-1.0 Hz. (e) Snapshots showing the morphology evolution of the droplet in an extraction-reinjection, [PA_3/Fe(III)] = 0.10 mg mL^{-1}, [NH_2-PDMS-NH_2] = 1.0 mg mL^{-1}.

Since the presence of the catechol-Fe^{3+} coordination bond and the imine bond usually allows reversible formation and disruption of the resultant assemblies under various kinds of stimuli, the responsiveness of supramolecular polymer networks was investigated by using four different stimuli: pH, redox, competing ligand and temperature. As shown in Figure 4a-f, a inverted pendant droplet is generated by injecting a toluene solution of NH_2-PDMS-NH_2 into an aqueous solution of PA_3/Fe(III), then the volume of the droplet is reduced to compress the interfacial assemblies, forming a jammed supramolecular polymer network at the interface. With the addition of HCl to the aqueous solution to decrease the pH, the wrinkles on the droplet gradually disappear, indicating the dissociation of catechol-Fe^{3+} coordination bond and imine bond, leading to a depolymerization of the supramolecular polymer networks, transforming the "solid-like" assembly into a "liquid-like" assembly (Figure 4a-b and Video S5). Similar behavior can be seen by adding $NaBH_4$ or ethylene diamine tetraacetic acid (EDTA, Figure S10) to the aqueous phase, where $NaBH_4$ is used as a reducing agent to degrade the PA_3/Fe(III) cross-linker via the reduction of Fe(III) to Fe(II) or Fe, and EDTA is used as a stronger chelating agent to coordinate with Fe^{3+} (Figure 4c-f, Video S6-S7). [23, 25] Also, by adjusting the amount of $NaBH_4$ or EDTA, the degree of disassembly of the supramolecular polymer networks can be effectively controlled, as evidenced by the varied interfacial tension and surface coverage (Figure S11-S12). Moreover, since the strength of catechol-Fe^{3+} coordination bond can be influenced by temperature, the thermal responsiveness of supramolecular polymer networks was investigated from 25 to 85 °C.[23] As shown in Figure 4g-h and Figure S13 (Video S8), when the temperature is increased to 75 °C, the pendant droplet with a jammed supramolecular polymer networks relaxes within one minute, indicating the disassociation of the catechol-Fe^{3+} coordination bond at high temperature. To show that the relaxation of the interfacial assembly is due to the disassociation of catechol-

Fe^{3+} coordination bond rather than an imine bond exchange, a control experiment was performed by dissolving branched polyethyleneimine (PEI) in water and a small molecule aldehyde (TBZ) in toluene (Figure S14). In this case, interfacial assemblies are formed by the bonding between PEI and TBZ and, when the temperature is increased to 75 °C, the droplet encapsulated with jammed interfacial assemblies cannot fully relax but remains in a nonequilibrium shape, indicating the imine bond exchange does not occur at this temperature (Figure S15).

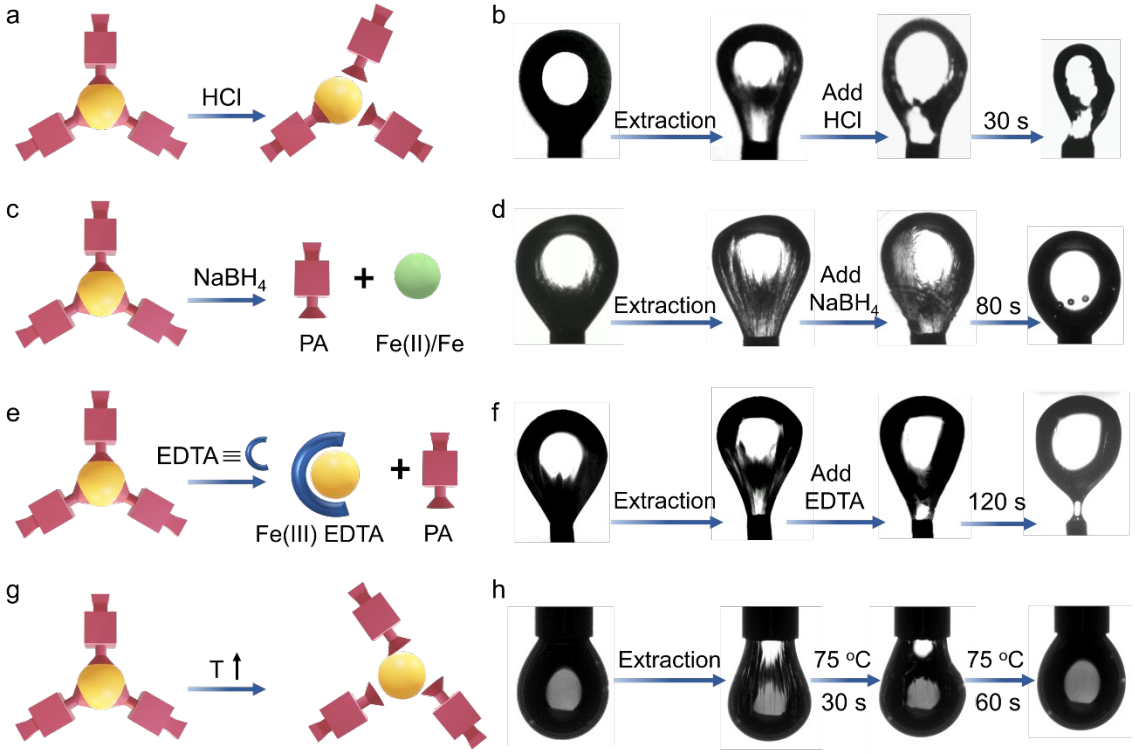

Figure 4. (a, c, e, g) Schematics showing the disassociation of catechol-Fe^{3+} coordination bond by using different stimuli including pH, redox, competing ligand and temperature. (b, d, f) Morphology evolution of the pendant droplet with jammed supramolecular polymer networks at the interface after inducing HCl, $NaBH_4$ or EDTA in the aqueous phase. (h) Morphology evolution of the pendant droplet with jammed supramolecular polymer networks at the interface

after the temperature is increased to 75 °C. [PA_3/Fe(III)] = 0.50 mg mL^{-1}; [NH_2-PDMS-NH_2] = 5.0 mg mL^{-1}; [HCl] = 0.1 mol L^{-1}, [$NaBH_4$] = 4.0 mg mL^{-1}; [EDTA] = 1.0 mg mL^{-1}.

Supramolecular polymer networks can also be constructed at the interface of emulsion droplets by vigorously homogenizing a aqueous solution containing PA_3/Fe(III) and a toluene solution containing NH_2-PDMS-NH_2 (Figure 5a). No stable emulsions are produced when using only PA_3/Fe(III) or NH_2-PDMS-NH_2 as the emulsifier. As shown in Figure 5a and Figure S16-S17, water-in-oil emulsions are produced at a constant water/toluene volume ratio of 1/5 and, by varying the concentration of either PA_3/Fe(III) or NH_2-PDMS-NH_2, the size of emulsion droplets can be well-controlled. Taking advantage of the multi-responsiveness of supramolecular polymer networks at the interface, the demulsification process can be easily achieved by adding the aqueous solution of HCl, $NaBH_4$ or EDTA to the emulsion systems, or, by increasing the temperature to 75 °C, where the encapsulated Rhodamine B in the emulsion droplets is released to the toluene phase (Figure 5b-e).

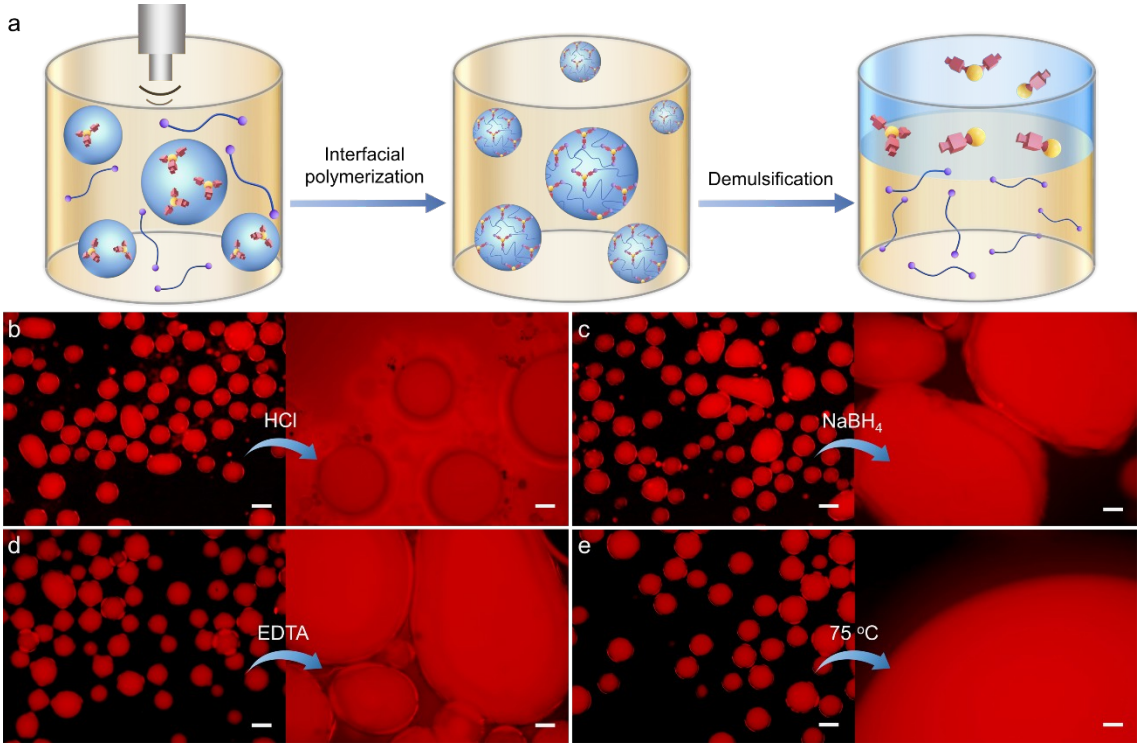

Figure 5. (a) Schematics showing the supramolecular polymerization of PA_3/Fe(III) and NH_2-PDMS-NH_2 at the interface of emulsion droplets. (b-e) Fluorescence microscopy images showing the demulsification processes of water-in-oil emulsions triggered by pH, $NaBH_4$, EDTA and temperature; [PA_3/Fe(III)] = 0.50 mg mL^{-1}, [NH_2-PDMS-NH_2] = 5.0 mg mL^{-1}, scale bar: 100 μm.

Finally, by using a flat oil-water interface as a template, large-scale, defect-free 2D Janus films can be prepared and transferred to a polytetrafluoroethylene (PTFE) support, producing a composite membrane that can be used for nanofiltration applications (Figure 6a and Figure S18). Figure 6b-c shows the optical images of 2D films prepared at the toluene-water interface and the resultant composite membrane. X-ray photoelectron spectroscopy (XPS) of the films exhibit three characteristic peaks at 532.3 eV, 400.3 eV, 284.3 eV assigned to O1s, N1s and C1s,

respectively. The C 1s spectrum can be deconvoluted into two peaks centered at 284.8 and 286.3 eV corresponding to C-C and C=N, and the N 1s spectrum can be deconvoluted into two peaks centered at 400.0 and 401.5 eV corresponding to C=N and unreacted NH_2, confirming the imine bond formation (Figure S19).[38] Figure 6d and Figure S20 show the atomic force microscopy (AFM) image and the height profile of films transferred onto a silicon wafer. By fixing the concentration of PA_3/Fe(III) at 0.50 mg mL^{-1} and varying the concentration of NH_2-PDMS-NH_2 from 2.0 to 10 mg mL^{-1}, a slight increase in the film thickness from 300 to 330 nm is observed, indicating that, after the initial rapid formation of film, the interfacial polymerization shifts to a slower growth stage as the initial film hinders the diffusion of the NH_2-PDMS-NH_2 to the reaction site.[39] However, the roughness of the film increases significantly, from 5.1 to 24.8 nm, with the increase of NH_2-PDMS-NH_2 concentration (Figure S21), which can be attributed to the faster reaction kinetics accompanied by more rapid heat evolution from the interfacial polymerization reaction.[40] Owing to the increased thickness and crumpled nature of the film (PA_3/Fe(III)-0.50&NH_2-PDMS-NH_2-10), decreased permeabilities of water and common polar/nonpolar solvents are realized in the resultant composite membranes (Figure 6e).[41] Filtration experiments were performed by using different organic dye molecules, including negatively charged methyl orange (MO, M_w = 327.33 g mol^{-1}), positively charged Rhodamine B (Rh B, M_w = 479.01 g mol^{-1}), neutral Congo Red (CR, M_w =696.66 g mol^{-1}) and negatively charged Evans Blue (EB, M_w = 960.81 g mol^{-1}), and all the film-based composite membranes showed a high rejection of EB (>99%) under 0.8 bar pressure (Figure 6f and Figure S22).

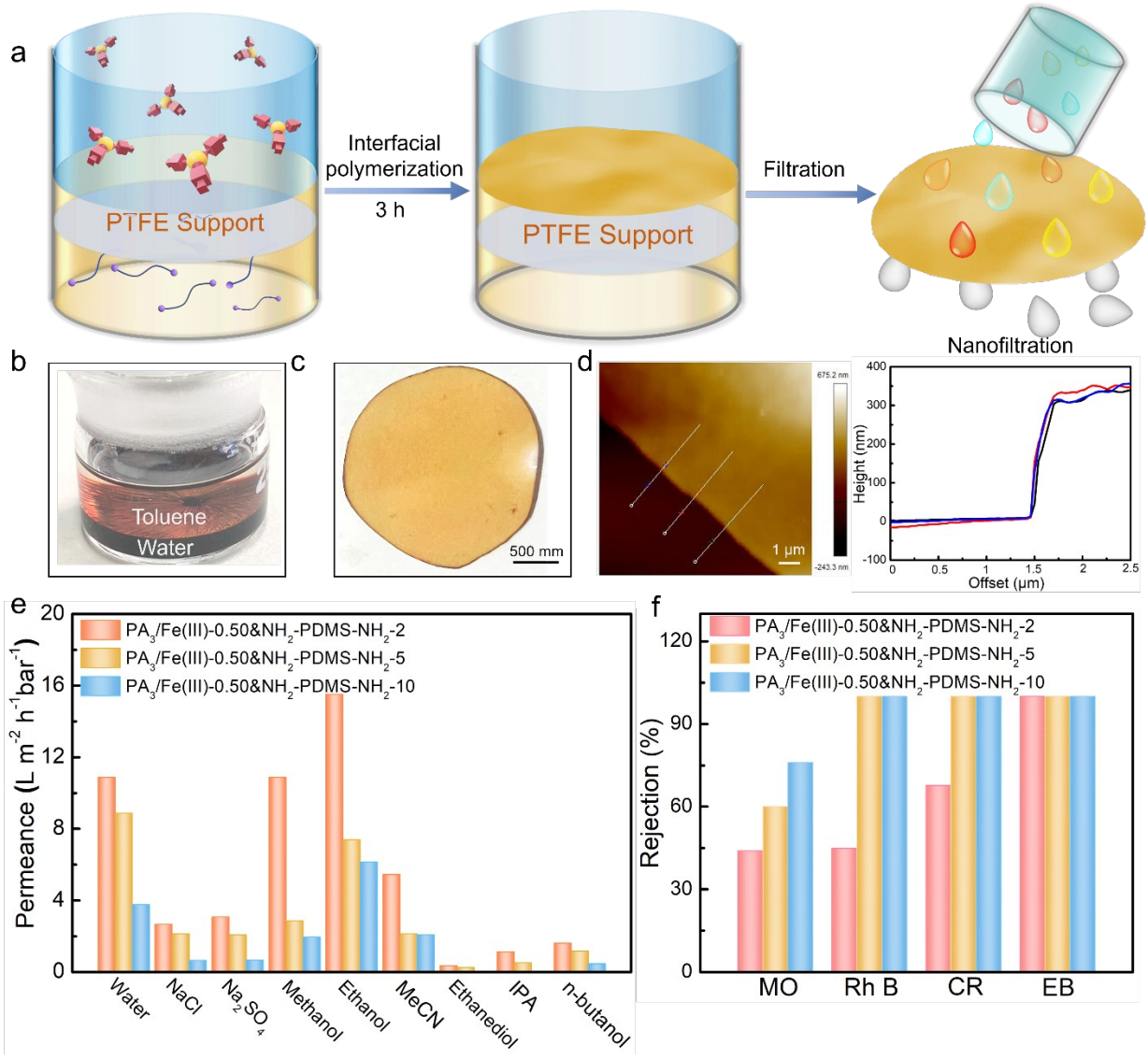

Figure 6. (a) Schematics showing the preparation of 2D film and resultant composite membrane. (b-c) Optical images showing the prepared 2D film and resultant composite membrane. (d) AFM height image and height profile (corresponding to the line drawn on the image) of films; [PA_3/Fe(III)] = 0.50 mg mL^{-1}, [NH_2-PDMS-NH_2]= 5.0 mg mL^{-1}. (e) Permeance and (f) rejection performance of resultant composite membrane.

Conclusion

In summary, by using the interfacial reaction between catechol-Fe^{3+} complexes and NH_2-PDMS-NH_2, we have demonstrated the design and preparation of linear supramolecular polymers and supramolecular polymer networks at the oil-water interface. In comparison to linear supramolecular polymers, supramolecular polymer networks show higher mechanical strength, allowing the structuring of liquids into highly non-equilibrium shapes. By using pH, redox, EDTA and temperature as stimuli, the depolymerization of the supramolecular polymer networks can be easily achieved at the water–oil interface. In addition, application of supramolecular polymer network-based 2D films for nanofiltration is investigated. This work enriches the field of supramolecular polymerization and provides insight into the fabrication of supramolecular polymers with tailor-made architecture and function.

ASSOCIATED CONTENT

Supporting Information.

The Supporting Information is available free of charge on the ACS Publications website at DOI:

Experimental section including materials, characterization, and additional experimental details (PDF).

Video S1: The morphology evolution of droplet of supramolecular polymer networks in non-equilibrium state (MP4)

Video S2: The morphology evolution of droplet of supramolecular linear polymers in non-equilibrium state (MP4)

Video S3: Droplets of supramolecular polymer networks in a repeated squeezing experiment (MP4)

Video S4: Droplets of supramolecular linear polymers in a repeated squeezing experiment (MP4)

Video S5: Disassembly of supramolecular polymer networks by adding HCl (MP4)

Video S6: Disassembly of supramolecular polymer networks by adding $NaBH_4$ (MP4)

Video S7: Disassembly of supramolecular polymer networks by adding EDTA (MP4)

Video S8: Disassembly of supramolecular polymer networks at 75 °C (MP4)

AUTHOR INFORMATION

Corresponding Author

*E-mail: shisw@mail.buct.edu.cn (S. Shi)

Orcid

Shaowei Shi: 0000-0002-9869-4340

Notes

The authors declare no competing financial interest.

ACKNOWLEDGMENT

This work was supported by the National Natural Science Foundation of China (52173018) and Beijing Natural Science Foundation (2222071). TPR was supported by the U.S. Department of Energy, Office of Science, Office of Basic Energy Sciences, Materials Sciences and Engineering

Division under Contract No. DE-AC02-05-CH11231 within the Adaptive Interfacial Assemblies Towards Structuring Liquids program (KCTR16).

Conflict of Interest

The authors declare no conflict of interest.

REFERENCES

1. Fouquey, C.; Lehn, J.-M.; Levelut, A.-M., Molecular recognition directed self-assembly of supramolecular liquid crystalline polymers from complementary chiral components. *Advanced Materials* **1990,** *2* (5), 254-257.

2. L. Brunsveld, B. J. B. F., E. W. Meijer, and R. P. Sijbesma, Supramolecular Polymers. *Chem. Rev.* **2001,** *101*, 4071-4097.

3. Lehn, J.-M., Supramolecular polymer chemistry: scope and perspectives. *Polymer International* **2002,** *51* (10), 825-839.

4. Huang, F.; Scherman, O. A., Supramolecular polymers. *Chem Soc Rev* **2012,** *41* (18), 5879-80.

5. Yang, L.; Tan, X.; Wang, Z.; Zhang, X., Supramolecular Polymers: Historical Development, Preparation, Characterization, and Functions. *Chem Rev* **2015,** *115* (15), 7196-239.

6. Hashim, P. K.; Bergueiro, J.; Meijer, E. W.; Aida, T., Supramolecular Polymerization: A Conceptual Expansion for Innovative Materials. *Progress in Polymer Science* **2020,** *105*.

7. Sun, P.; Qin, B.; Xu, J.-F.; Zhang, X., Supramonomers for controllable supramolecular polymerization and renewable supramolecular polymeric materials. *Progress in Polymer Science* **2022,** *124*.

8. T. Aida, E. W. M., S. I. Stupp, Functional Supramolecular Polymers. *Science* **2012,** *335*, 815-817.

9. Yan, X.; Wang, F.; Zheng, B.; Huang, F., Stimuli-responsive supramolecular polymeric materials. *Chem Soc Rev* **2012,** *41* (18), 6042-65.

10. Li, S. L.; Xiao, T.; Lin, C.; Wang, L., Advanced supramolecular polymers constructed by orthogonal self-assembly. *Chem Soc Rev* **2012,** *41* (18), 5950-68.

11. Wei, P.; Yan, X.; Huang, F., Supramolecular polymers constructed by orthogonal self-assembly based on host-guest and metal-ligand interactions. *Chem Soc Rev* **2015,** *44* (3), 815-32.

12. Winter, A.; Schubert, U. S., Synthesis and characterization of metallo-supramolecular polymers. *Chem Soc Rev* **2016,** *45* (19), 5311-57.

13. Qin, B.; Yin, Z.; Tang, X.; Zhang, S.; Wu, Y.; Xu, J.-F.; Zhang, X., Supramolecular polymer chemistry: From structural control to functional assembly. *Progress in Polymer Science* **2020,** *100*.

14. Peng, H.-Q.; Zhu, W.; Guo, W.-J.; Li, Q.; Ma, S.; Bucher, C.; Liu, B.; Ji, X.; Huang, F.; Sessler, J. L., Supramolecular polymers: Recent advances based on the types of underlying interactions. *Progress in Polymer Science* **2023,** *137*.

15. Zheng, Y.; Yu, Z.; Parker, R. M.; Wu, Y.; Abell, C.; Scherman, O. A., Interfacial assembly of dendritic microcapsules with host-guest chemistry. *Nat. Commun.* **2014,** *5*, 5772.

16. Qin, B.; Zhang, S.; Song, Q.; Huang, Z.; Xu, J. F.; Zhang, X., Supramolecular Interfacial Polymerization: A Controllable Method of Fabricating Supramolecular Polymeric Materials. *Angew Chem Int Ed Engl* **2017,** *56* (26), 7639-7643.

17. Qin, B.; Zhang, S.; Huang, Z.; Xu, J.-F.; Zhang, X., Supramolecular Interfacial Polymerization of Miscible Monomers: Fabricating Supramolecular Polymers with Tailor-Made Structures. *Macromolecules* **2018,** *51* (5), 1620-1625.

18. Qin, B.; Xu, J. F.; Zhang, X., Supramolecular Polymerization at Interfaces. *Langmuir* **2022,** *38* (14), 4157-4163.

19. Haeshin Lee, S. M. D., William M. Miller, Phillip B. Messersmith, Mussel-Inspired Surface Chemistry for Multifunctional Coatings. *Science* **2007,** *318*, 426-430.

20. Emmanouela Filippidi, T. R. C., Claus D. Eisenbach,; J. Herbert Waite; Jacob N. Israelachvili; B. Kollbe Ahn; Valentine, M. T., Toughening elastomers using musselinspired iron-catechol complexes. *Science* **2017,** *358*, 502–505.

21. Zhang, C.; Wu, B.; Zhou, Y.; Zhou, F.; Liu, W.; Wang, Z., Mussel-inspired hydrogels: from design principles to promising applications. *Chem Soc Rev* **2020,** *49* (11), 3605-3637.

22. Chen, J.; Zeng, H., Mussel-Inspired Reversible Molecular Adhesion for Fabricating Self-Healing Materials. *Langmuir* **2022,** *38* (43), 12999-13008.

23. Sen Hou, P. X. M., Stimuli-Responsive Supramolecular Hydrogels with High Extensibility and Fast Self-Healing via Precoordinated MusselInspired Chemistry. *Chem. Mater.* **2015,** *27*, 2651–2655.

24. Kim, B. J.; Cheong, H.; Hwang, B. H.; Cha, H. J., Mussel-Inspired Protein Nanoparticles Containing Iron(III)-DOPA Complexes for pH-Responsive Drug Delivery. *Angew Chem Int Ed Engl* **2015,** *54* (25), 7318-22.

25. Li, M.; Wang, H.; Hu, J.; Hu, J.; Zhang, S.; Yang, Z.; Li, Y.; Cheng, Y., Smart Hydrogels with Antibacterial Properties Built from All Natural Building Blocks. *Chemistry of Materials* **2019,** *31* (18), 7678-7685.

26. Liang, R.; Yu, H.; Wang, L.; Wang, N.; Amin, B. U., NIR Light-Triggered Shape Memory Polymers Based on Mussel-Inspired Iron–Catechol Complexes. *Adv. Funct. Mater.* **2021**, 2102621.

27. Yuqing Liang, Z. L., Ying Huang, Rui Yu, and Baolin Guo, Dual-Dynamic-Bond Cross-Linked Antibacterial Adhesive Hydrogel Sealants with On-Demand Removability for Post-WoundClosure and Infected Wound Healing. *ACS Nano* **2021,** *15*, 7078-7093.

28. Sun, P.; Mei, S.; Xu, J. F.; Zhang, X., A Bio-Based Supramolecular Adhesive: Ultra-High Adhesion Strengths at both Ambient and Cryogenic Temperatures and Excellent Multi-Reusability. *Adv Sci* **2022,** *9* (28), e2203182.

29. Shannon, D. P.; Moon, J. D.; Barney, C. W.; Sinha, N. J.; Yang, K. C.; Jones, S. D.; Garcia, R. V.; Helgeson, M. E.; Segalman, R. A.; Valentine, M. T.; Hawker, C. J., Modular

Synthesis and Patterning of High-Stiffness Networks by Postpolymerization Functionalization with Iron-Catechol Complexes. *Macromolecules* **2023,** *56* (6), 2268-2276.

30. Niels Holten-Andersena; , M. J. H. H. B., Bruce P. Leed , Phillip B. Messersmith, Ka Yee C. Leea, and J. Herbert Waite, pH-induced metal-ligand cross-links inspired bymussel yield self-healing polymer networkswith near-covalent elastic moduli. *PNAS* **2011,** *108* (7), 2651–2655.

31. Stoddart, M. E. B. a. J. F., Dynamic imine chemistry. *Chem. Soc. Rev.* **2012,** *41*, 2003–2024.

32. Chen, D.; Sun, Z.; Russell, T. P.; Jin, L., Coassembly Kinetics of Graphene Oxide and Block Copolymers at the Water/Oil Interface. *Langmuir* **2017,** *33* (36), 8961-8969.

33. Zhang, B.; Zhang, P.; Zhang, H.; Yan, C.; Zheng, Z.; Wu, B.; Yu, Y., A Transparent, Highly Stretchable, Autonomous Self-Healing Poly(dimethyl siloxane) Elastomer. *Macromol Rapid Commun* **2017,** *38* (15).

34. Guo-Yong Chai, W. B. K., Formation and characterization of polyamide membranes via interfacial polymerization. *Journal of Membrane Science* **1994,** *93*, 175-192.

35. Freger, V., Nanoscale Heterogeneity of Polyamide Membranes Formed by Interfacial Polymerization. *Langmuir* **2003,** *19* (11), 4791-4797.

36. Shi, S.; Russell, T. P., Nanoparticle Assembly at Liquid–Liquid Interfaces. *Adv. Mater.* **2018,** *30* (1800714).

37. Forth, J.; Kim, P. Y.; Xie, G.; Liu, X.; Helms, B. A.; Russell, T. P., Building Reconfigurable Devices Using Complex Liquid-Fluid Interfaces. *Adv. Mater.* **2019,** *31* (18), 1806370.

38. Tiwari, K.; Sarkar, P.; Modak, S.; Singh, H.; Pramanik, S. K.; Karan, S.; Das, A., Large Area Self-Assembled Ultrathin Polyimine Nanofilms Formed at the Liquid-Liquid Interface Used for Molecular Separation. *Adv Mater* **2020,** *32* (8), 1905621.

39. Khorshidi, B.; Thundat, T.; Fleck, B. A.; Sadrzadeh, M., A Novel Approach Toward Fabrication of High Performance Thin Film Composite Polyamide Membranes. *Scientific Reports* **2016,** *6* (1).

40. Santanu Karan, Z. J., Andrew G. Livingston, Sub-10 nm polyamide nanofilms with ultrafast solvent transport for molecular separation. *Science* **2015,** *348* (6214).

41. Lalia, B. S.; Kochkodan, V.; Hashaikeh, R.; Hilal, N., A review on membrane fabrication: Structure, properties and performance relationship. *Desalination* **2013,** *326*, 77-95.